Parkinsonism and Related Disorders xxx (2018) 1–7

Contents lists available at ScienceDirect

Parkinsonism and Related Disorders

journal homepage: www.elsevier.com/locate/parkreldis

Diagnostic potential of dentatorubrothalamic tract analysis in progressive supranuclear palsy

Morinobu Seki [a, b, *], Klaus Seppi [a, b], Christoph Mueller [a], Thomas Potrusil [a, b], Georg Goebel [c], Eva Reiter [a], Michael Nocker [a], Ruth Steiger [b, d], Matthias Wildauer [b, d], Elke R. Gizewski [b, d], Gregor K. Wenning [a], Werner Poewe [a], Christoph Scherfler [a, b]

[a] Department of Neurology, Medical University of Innsbruck, Austria
[b] Neuroimaging Research Core Facility, Medical University of Innsbruck, Austria
[c] Department of Medical Statistics, Informatics and Health Economics, Medical University of Innsbruck, Austria
[d] Department of Neuroradiology, Medical University of Innsbruck, Austria

ARTICLE INFO

Article history:
Received 3 May 2017
Received in revised form
4 January 2018
Accepted 2 February 2018

Keywords:
Richardson's syndrome
Progressive supranuclear palsy-parkinsonism
Dentatorubrothalamic tract
Diffusion tensor imaging
Diagnostic marker

ABSTRACT

Background: The differentiation of progressive supranuclear palsy-parkinsonism (PSP-P) from Parkinson's disease (PD) remains a major clinical challenge.
Objectives: To evaluate the diagnostic potential of observer-independent assessments of microstructural integrity within infratentorial brain regions to differentiate PSP-Richardson's syndrome (PSP-RS), PSP-P and PD.
Methods: 3T MRI parameters of mean diffusivity, fractional anisotropy, grey and white matter volumes from patients with PSP-RS (n = 12), PSP-P (n = 12) and mean disease duration of 2.4 ± 1.7 years were compared with PD patients (n = 20) and healthy controls (n = 23) by using statistical parametric mapping and the spatially unbiased infratentorial template. Subsequently MRI measurements of the dentatorubrothalamic tract were determined observer-independently by a validated probabilistic infratentorial atlas. The impairment of gait and postural stability was evaluated by a sum-score derived from the Unified Parkinson Disease Rating Scale.
Results: Significant mean diffusivity increases, fractional anisotropy decreases and corresponding volume loss were localized in mesencephalic tegmentum, superior cerebellar peduncle, decussation of superior cerebellar peduncle and dentate nucleus in PSP-RS and PSP-P compared to PD and healthy controls. Altered microstructural integrity of the dentatorubrothalamic tract in PSP-RS was significantly more pronounced compared to PSP-P and correlated significantly with the gait and postural stability sum-score. Linear discriminant analysis identified diffusion tensor imaging measures of the dentatorubrothalamic tract and the gait and postural stability sum-score to classify correctly 95.5% of PRP-RS, PSP-P and PD patients.
Conclusions: Observer-independent analysis of microstructural integrity within the dentatorubrothalamic tract in combination with assessments of gait and postural stability differentiate PSP-P from PSP-RS and PD in early to moderately advanced stages.

1. Introduction

Progressive supranuclear palsy (PSP) is a neurodegenerative disorder pathologically defined by the accumulation of tau protein and neuropil threads mainly in the pallidum, subthalamic nucleus, red nucleus, pontine tegmentum, substantia nigra and dentate nucleus [1–3]. The current operational clinical diagnostic criteria of PSP require the clinical features of supranuclear gaze palsy or slowed vertical saccades and frequent falls in the first year of disease due to postural instability and this clinical presentation has been referred to as Richardson's syndrome (PSP-RS) [4,5]. However, sensitivity of the criteria is low due to the delayed evolution or even the absence of those signs in a substantial proportion of patients [5–8]. Based on a clinico-pathological series of 103 PSP cases,

* Corresponding author. Department of Neurology, Medical University of Innsbruck, Anichstrasse 35, A-6020 Innsbruck, Austria.
E-mail address: mseki-neuro@umin.ac.jp (M. Seki).

https://doi.org/10.1016/j.parkreldis.2018.02.004
1353-8020/

Williams and colleagues were able to delineate a distinct PSP phenotype with prominent parkinsonian features, with moderate initial therapeutic response to levodopa and absence of gaze palsy or falls within the first two years of the disease and suggested the term PSP-parkinsonism (PSP-P) [5]. Since then, the clinical spectrum of PSP presentations has enlarged further [8] and novel diagnostic criteria for PSP have been suggested to reflect this phenotypic diversity [9].

Nonetheless, the differentiation of PSP-P from Parkinson's disease (PD) patients remains a major clinical challenge [10]. Recently, MRI studies applying advanced volumetric and diffusion tensor imaging analysis revealed significant signal alterations in the midbrain, superior cerebellar peduncle (SCP), the corpus callosum and the internal capsules of PSP-RS compared to PSP-P and PD on the group level and thus hold promise as diagnostic tools [11–13]. However, there have been few attempts to distinguish among those entities on the single subject level using MRI in early disease stages [14,15].

By applying dedicated voxel-based analysis to the infratentorial brain area, the present study was conducted first to characterize objectively assessable MRI markers of mean diffusivity and fractional anisotropy in early to moderately advanced disease stages of PSP-RS, PSP-P and PD [16,17]. Secondly, derived from the results obtained at the group level, MRI metrics of the dentatorubrothalamic tract (DRTT) were investigated by using a validated probabilistic infratentorial atlas upon its potential to differentiate PSP-RS, PSP-P and PD on the individual level.

2. Methods

2.1. Subjects

Twelve patients with PSP-RS, 12 patients with PSP-P and 26 patients with PD were recruited consecutively at our centre. MRI was performed within 1 month of the initial clinical examination. To be eligible, participants had to fulfill consensus operational criteria of probable PSP and PD made by two movement disorders specialists at clinical follow-up of at least 24 months [4,18–20]. When falls, supranuclear gaze palsy, abnormal vertical saccadic eye movements and cognitive decline were the predominant clinical features in the first two years of the disease, patients were classified as PSP-RS [5,19]. In contrast, patients presenting with asymmetric bradykinesia, rigidity, or tremor and a positive response to L-dopa and no evidence of prominent postural instability with falls, supranuclear gaze palsy or abnormal vertical saccadic eye movements in the first two years, were classified as PSP-P. Further inclusion criteria, all anchored at the time of MRI, included disease duration of less than 6 years and age of 50–75 years. Motor disability was assessed in all patients in OFF drug states using part III of the Unified Parkinson's Disease Rating Scale (UPDRS) and the Hoehn and Yahr stage. To evaluate the severity of postural instability and gait disturbance, a sum of the following items from the UPDRS part II and III was calculated (UPDRS gait and postural stability sum-score); II13 (Falling), II15 (Walking), III29 (Gait) and III30 (Postural stability). 20 out of 26 consecutively recruited PD patients were matched for gender, age and disease duration. Twenty-three healthy individuals with no signs of central nervous system disorders and a Mini-Mental State Examination score of >28 served as age and gender-matched control group. Participants with white matter lesion of grade 2 and 3 in Fazekas scale [21], space-occupying lesions, or motion artefacts were excluded. Fazekas scale quantifies the severity of white matter hyperintensity lesions on MR images, which are usually attributed to chronic small vessel ischemia. Grade 2 corresponds to larger white matter lesions that are beginning to become confluent and grade 3 corresponds to large confluent lesions. The study was approved by the Ethics Committee of the Medical University of Innsbruck. The subjects' written informed consent was obtained according to the Declaration of Helsinki.

2.2. MRI data acquisition

All MRI measurements were performed on a 3.0 T whole-body MR scanner (MagnetomVerio, Siemens, Erlangen, Germany) equipped with a twelve-channel head coil. All participants underwent the same MRI protocol, including whole-brain T1-weighted, fluid-attenuated inversion-recovery, T2 and proton density-weighted as well as diffusion tensor imaging (DTI). The MRI parameters for the coronal T1-weighted 3D magnetization prepared rapid gradient echo (3D-MPRAGE) were TR 1800 ms; TE 2.18 ms; inversion time, 900 ms; slice thickness, 1.2 mm; matrix, 256×204 pixels; number of excitations, 1; flip angle, 9°; field of view, 220×165 mm. The DTI data were acquired using spin-echo echo-planar imaging (echo time/repetition time = 83/8200 ms, bandwidth = 1596 Hz/pixel; matrix size 116×116; 45 axial slices; voxel size, $2 \times 2 \times 3$ mm^3) with 20 diffusion gradient directions with a b-value of 1000 s/mm^2 and one reference image with b = 0.

2.3. Imaging post processing

To avoid a priori assumptions through region of interest (ROI) analysis on brain areas of potential interests, we applied a voxel-based analysis of entire infrantentorial region to multimodal mean diffusivity (MD), fractional anisotropy (FA) and volumetric measures of the grey and white matter compartments [16,17]. Grey and white matter volume, MD and FA measures were subjected to statistical parametric mapping (SPM, Wellcome Department of Cognitive Neurology, London, UK [16]). The software package SPM12 implemented in Matlab 7.8 (Mathsworks Inc., Sherborn, MA) was used to preprocess and analyze MRI data. The infratentorial structures (i.e., the cerebellum and brainstem) were isolated from the supratentorial structures on the MPRAGE images and the segmented grey matter (GM) and white matter (WM) images were generated using the SUIT toolbox v2.7 [17]. The cropped images were then normalized onto the spatially unbiased high-resolution infratentorial template (SUIT), and the resulting transformation parameters were applied to the segmented volumetric images. A modulation of the segmentation map using the Jacobian determinants was undertaken to compensate for volume changes during the normalization. The deformation map generated in the normalization step was also applied to the previously coregistered MD and FA images. Finally, the normalized infratentorial images were smoothed with a 4-mm full-width half-maximum Gaussian kernel in order to accommodate inter-individual anatomic variability and to improve signal to noise ratios for the statistical analysis. A masking threshold of 10% of the lower image signal was applied to reduce signal noise. For DTI analysis, age was included as a covariate. For voxel based morphometry, age and total intracranial volume were entered as covariates. Subsequently a previously validated automated, atlas-based ROI analysis of the infratentorial brain region including the DRTT and pontocerebellar tract (PCT), which is independent from our categorical SPM analysis, was evaluated upon its applicability in clinical practice [22]. Observer-independently defined ROI's were transformed to individual subject's space using the deformation parameters obtained from the normalization step. Individual subject's volume and DTI metrics of the DRTT and PCT were extracted, adjusted for total intracranial volume and correlated to demographic and clinical parameters including semiquantitative assessments of gait and postural stability. Supplementary Fig. 1 shows a sample of the ROIs of the DRTT

Please cite this article in press as: M. Seki, et al., Diagnostic potential of dentatorubrothalamic tract analysis in progressive supranuclear palsy, Parkinsonism and Related Disorders (2018), https://doi.org/10.1016/j.parkreldis.2018.02.004

and PCT superimposed on the individual's FA image.

2.4. Statistical analysis

Demographic data are presented as frequencies and means (±SD). The binominal test was performed to test for the distribution of gender. One-way analysis of variance (ANOVA) with post-hoc Tukey's test was applied for group comparison of age, disease duration, UPDRS part III, UPDRS gait and postural stability sum-score, Hoehn & Yahr stage, ROI values and asymmetry index. Between-group comparisons of grey and white matter segments, as well as MD and FA maps were assessed using one-way ANOVA design with $p < 0.001$ as level of significance. The family-wise error (FWE) at a threshold of $p < 0.05$ was applied to correct for multiple comparisons at the voxel-cluster level.

The relationship between clinical parameters including disease duration, UPDRS part III score and UPDRS gait and postural stability sum-score and MRI measurements was investigated using Pearson's correlation statistics. To discriminate among groups, linear discriminant analysis (LDA) was performed using MD and FA metrics of the more affected side of the DRTT. Since the UPDRS gait and postural stability sum-score correlated selectively with MD measure of the DRTT of the PSP-PS group without showing a significant association across all patients' groups, this score was included to the LDA. For group membership, the same a priori probability was assumed for all cases. We used equal prevalences for each of the three disease entities ($p = 0.33$). A leave-one-out cross validation procedure was applied for computing the accuracy rate of the model. Statistical analysis was carried out using a commercial software package (SPSS 20.0, Surrey, UK).

3. Results

3.1. Clinical variables (Supplementary Table 1)

Gender, age and disease duration did not differ significantly among the PSP-RS, PSP-P, PD and healthy control (HC) groups. Compared to PD patients, the UPDRS gait and postural stability sum-score was significantly more affected in both PSP groups ($p < 0.001$).

3.2. Mean diffusivity and fractional anisotropy (Fig. 1a and b, Supplementary Tables 2 and 3)

SPM localized voxel clusters of significant MD increases and FA decreases in brain regions corresponding to the DRTT such as the decussation of SCP (DSCP), the bilateral SCPs, the dentate nucleus and the mesencephalic tegmentum of the PSP-RS group, as compared to the PD and HC groups ($p < 0.0001$). In the PSP-RS group significant MD increases were also evident in the

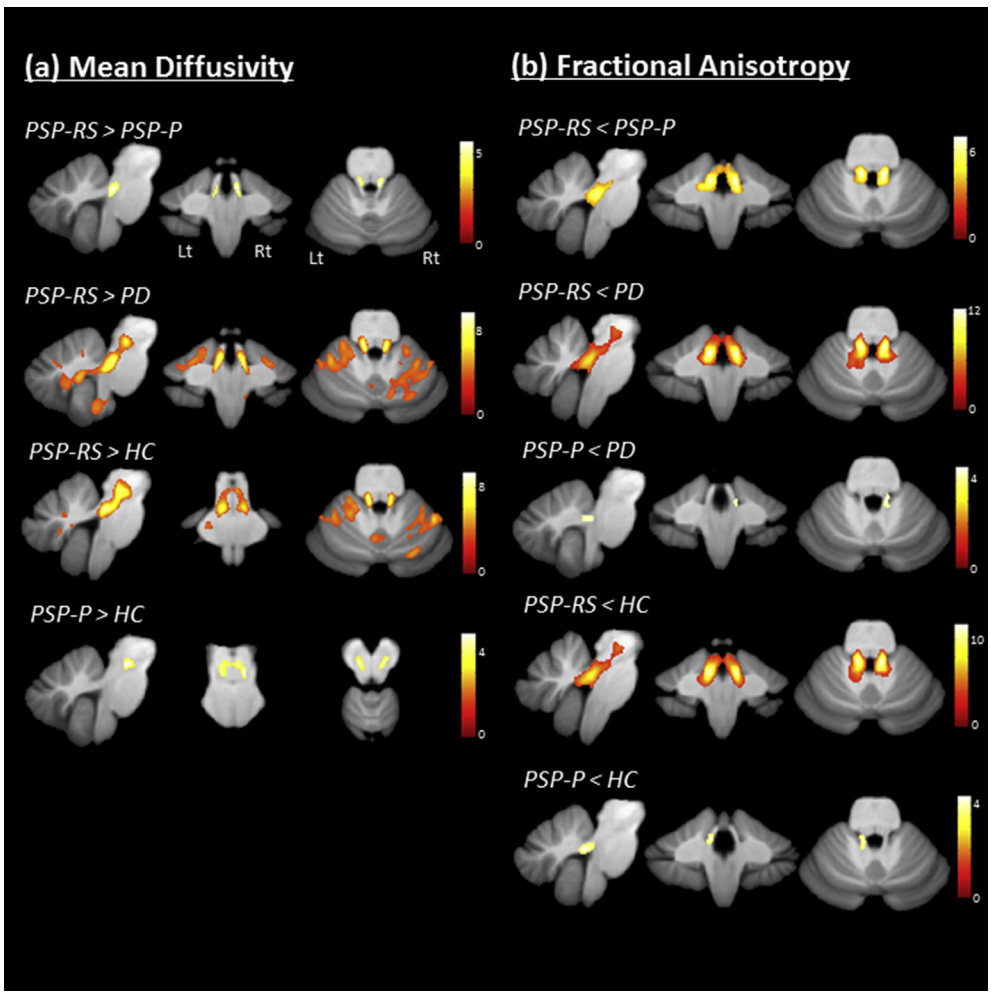

Fig. 1. Voxel-based analysis of diffusion tensor imaging (DTI) of the infratentorial brain regions in patients with Richardson's syndrome (PSP-RS), progressive supranuclear palsy-parkinsonism (PSP-P), Parkinson's disease (PD) and healthy controls (HC).
The images represent the regions showing significant increases of mean diffusivity (a) and decreases of fractional anisotropy (b) in the comparisons between the pairs of groups.

Please cite this article in press as: M. Seki, et al., Diagnostic potential of dentatorubrothalamic tract analysis in progressive supranuclear palsy, Parkinsonism and Related Disorders (2018), https://doi.org/10.1016/j.parkreldis.2018.02.004

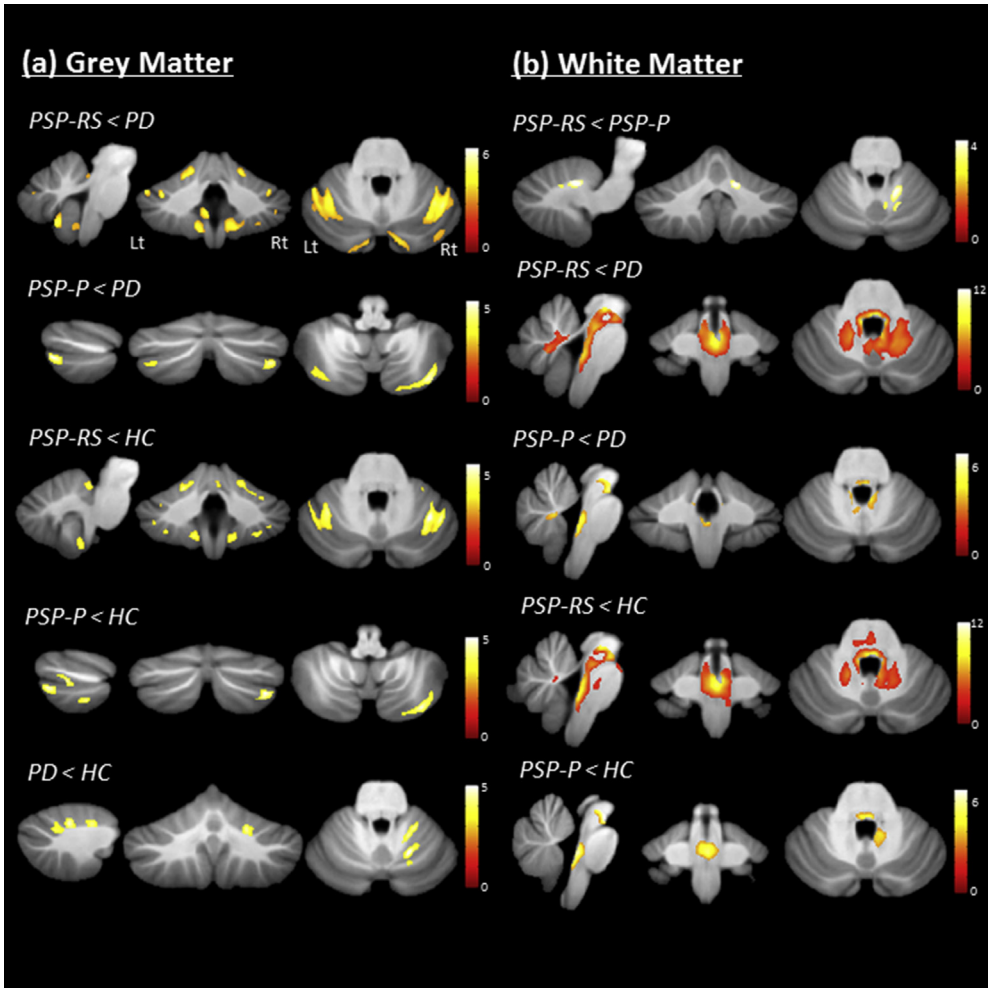

Fig. 2. Voxel-based morphometry of the infratentorial brain regions in patients with Richardson's syndrome (PSP-RS), progressive supranuclear palsy-parkinsonism (PSP-P), Parkinson's disease (PD) and healthy controls (HC).
The images represent the regions showing significantly decreased grey matter (a) and white matter (b) volumes in the comparisons between the pairs of groups.

cerebellar cortex and WM compared to the PD and HC groups and in the left middle cerebellar peduncle (MCP) compared to the HC group ($p < 0.0001$). Additionally PSP-P patients showed significant relative increases of MD in the mesencephalic tegmentum compared to the HC group ($p < 0.01$) as well as reduced FA in the SCP and the dentate nucleus compared to the PD and HC groups ($p < 0.05$). When comparing PSP-RS with PSP-P, MD values were significantly increased in the bilateral SCPs and the DSCP and FA values were significantly decreased in the bilateral SCPs, the dentate nucleus and the mesencephalic tegmentum of the former (MD $p < 0.05$; FA $p < 0.0001$).

3.3. Grey and white matter volume (Fig. 2a and b, Supplementary Tables 4 and 5)

In the PSP-RS and PSP-P groups significant GM reduction was evident in the cerebellar cortex compared to the PD and HC groups (PSP-RS $p < 0.0001$; PSP-P $p < 0.01$). Additionally in PD patients, significant GM reduction was found in the cerebellar cortex compared to the HC group ($p < 0.0001$).

Significant WM reductions were identified in the mesencephalic tegmentum, the DSCP, the bilateral SCPs, the dentate nucleus, the dorsal part of pons and the cerebellar WM of the PSP-RS and PSP-P groups compared to the PD and HC groups (PSP-RS $p < 0.0001$; PSP-P $p < 0.01$). Additionally, the PSP-RS group showed significant WM loss in the left MCP compared with the HC group ($p < 0.0001$) and in the cerebellar WM compared to the PSP-P group ($p < 0.05$).

3.4. Automated, atlas-based ROI analysis (Table 1)

Significantly increased MD and decreased FA values of the bilateral ROIs of the DRTT as well as the more affected side were observed in the PSP-RS, as compared to the PSP-P, PD and HC groups ($p < 0.001$). The PSP-P group also showed significantly increased MD values of the bilateral ROIs of the DRTT as well as the more affected side compared to the PD and HC groups ($p < 0.001$). Volume of the bilateral DRTTs and of the more affected side was significantly decreased in the PSP-RS ($p < 0.01$) and PSP-P groups ($p < 0.05$) compared to the PD and HC groups.

Significantly increased MD and decreased FA values of the bilateral ROIs and of the more affected side of the PCTs were observed in the PSP-RS, as compared to the PD ($p < 0.05$) and HC groups ($p < 0.01$). Additionally, significant volume loss of both PCTs was evident in the PSP-RS group compared to the HC group ($p < 0.05$).

3.5. Correlations of clinical assessments and MRI parameters (Supplementary Fig. 2)

In the PSP-RS group, significant, positive correlations were found between MD increases of the more affected side of the DRTT

Please cite this article in press as: M. Seki, et al., Diagnostic potential of dentatorubrothalamic tract analysis in progressive supranuclear palsy, Parkinsonism and Related Disorders (2018), https://doi.org/10.1016/j.parkreldis.2018.02.004

Table 1
Mean diffusivity (MD), fractional anisotropy (FA) and volumetric values of the dentatorubrothalamic tract and the pontocerebellar tract of patients with Richardson's syndrome (PSP-RS), progressive supranuclear palsy-parkinsonism (PSP-P), Parkinson's disease (PD) and healthy controls (HC).

	PSP-RS	PSP-P	PD	HC	ANOVA (p-value)
(a) The dentatorubrothalamic tract (DRTT)					
MD values [$mm^2 \cdot s^{-1}$]					
Mean of both sides	$1180.2 \pm 68.1^{***\dagger\dagger\dagger\ddagger\ddagger\ddagger}$	$1013.7 \pm 61.3^{***\dagger\dagger\dagger}$	920.8 ± 40.7	924.7 ± 37.5	<0.0001
More affected side	$1216.1 \pm 71.7^{***\dagger\dagger\dagger\ddagger\ddagger\ddagger}$	$1029.9 \pm 63.7^{***\dagger\dagger\dagger}$	941.4 ± 44.8	945.5 ± 39.4	<0.0001
Asymmetry index (%)	6.1 ± 3.9	3.5 ± 2.1	4.5 ± 2.5	4.5 ± 2.6	0.16
FA values [$mm^2 \cdot s^{-1}$]					
Mean of both sides	$397.5 \pm 37.6^{***\dagger\dagger\dagger\ddagger\ddagger\ddagger}$	477.7 ± 30.0	502.9 ± 23.9	500.6 ± 28.4	<0.0001
More affected side	$382.8 \pm 35.7^{***\dagger\dagger\dagger\ddagger\ddagger\ddagger}$	465.2 ± 37.8	489.9 ± 25.8	489.5 ± 30.2	<0.0001
Asymmetry index (%)	7.3 ± 4.0	5.9 ± 5.9	5.2 ± 3.3	4.5 ± 3.0	0.23
Volume [10^3]					
Mean of both sides	$0.83 \pm 0.12^{***\dagger\dagger}$	$0.86 \pm 0.13^{**\dagger}$	0.98 ± 0.13	1.01 ± 0.11	<0.001
More affected side	$0.79 \pm 0.12^{**\dagger\dagger}$	$0.81 \pm 0.13^{*\dagger}$	0.94 ± 0.13	0.95 ± 0.12	<0.001
Asymmetry index (%)	10.8 ± 6.0	11.0 ± 4.7	10.0 ± 3.6	11.9 ± 3.9	0.55
(b) The pontocerebellar tract (PCT)					
MD values [$mm^2 \cdot s^{-1}$]					
Mean of both sides	$776.8 \pm 34.2^{**\dagger}$	759.8 ± 27.6	748.5 ± 19.5	744.8 ± 24.0	<0.01
More affected side	$783.5 \pm 36.6^{**\dagger}$	764.8 ± 28.0	755.6 ± 21.7	751.2 ± 25.3	<0.05
Asymmetry index (%)	1.7 ± 1.5	1.5 ± 1.0	1.9 ± 1.2	1.8 ± 1.5	0.85
FA values [$mm^2 \cdot s^{-1}$]					
Mean of both sides	451.2 ± 26.2	466.0 ± 15.0	466.8 ± 21.2	467.7 ± 20.1	0.14
More affected side	443.6 ± 27.5	458.6 ± 18.1	458.1 ± 23.1	461.2 ± 22.3	0.18
Asymmetry index (%)	3.4 ± 2.3	3.5 ± 3.3	3.8 ± 2.3	2.8 ± 2.5	0.67
Volume [10^3]					
Mean of both sides	$7.88 \pm 0.54^{*}$	8.07 ± 0.88	8.51 ± 0.65	8.63 ± 0.57	<0.01
More affected side	$7.66 \pm 0.57^{*}$	7.77 ± 0.86	8.24 ± 0.65	8.36 ± 0.56	<0.01
Asymmetry index (%)	5.6 ± 5.7	7.4 ± 2.9	6.5 ± 2.8	6.4 ± 1.9	0.57

$^{*}p < 0.05$; $^{**}p < 0.01$; $^{***}p < 0.001$ versus HC.
$^{\dagger}p < 0.05$; $^{\dagger\dagger}p < 0.01$; $^{\dagger\dagger\dagger}p < 0.001$ versus PD.
$^{\ddagger\ddagger\ddagger}p < 0.001$ versus PSP-P
Values represent the means (±SD). For volume and FA values, the side of the regions with lower values was selected as more affected side. On the other hand, for MD values, the side of the regions with higher MD values was selected as more affected side. The more affected parameter was averaged within the group. The asymmetry index was calculated according to the formula: $[(a - b)/(a + b)] \times 2 \times 100$, where a and b represent the two different sides of the brain region.

Table 2
Diagnostic classification matrix, based on (a) regional diffusion tensor imaging values of the dentatorubrothalamic tract (DRTT) and (b) regional diffusion tensor imaging values of the DRTT and the UPDRS gait and postural stability sum-score.

(a)

Clinical classification	Predicted group by MD and FA values of the more affected side of the DRTT		
	PSP-RS	PSP-P	PD
PSP-RS (n = 12)	**11 (91.7%)**	1	0
PSP-P (n = 12)	0	**9 (75.0%)**	3
PD (n = 20)	0	3	**17(85.0%)**

(b)

Clinical classification	Predicted group by MD and FA values of the more affected side of the DRTT and the UPDRS gait and postural stability sum-score		
	PSP-RS	PSP-P	PD
PSP-RS (n = 12)	**11(91.7%)**	**1**	0
PSP-P (n = 12)	0	**11(91.7%)**	1
PD (n = 20)	0	0	**20 (100%)**

DRTT: dentatorubrothalamic tract, FA: fractional anisotropy, MD: mean diffusivity, PD: Parkinson's disease, PSP-P: progressive supranuclear palsy-parkinsonism, PSP-RS: Richardson's syndrome, UPDRS: Unified Parkinson's Disease Rating Scale.
The classification of subjects' mean diffusivity (MD) and fractional anisotropy (FA) values of more affected side of the DRTT with respect to their clinical diagnosis was calculated by linear discriminant analysis (Table 2a). The classification was also calculated when adding the UPDRS gait and postural stability sum-score to the model (Table 2b). Rows represent the clinical diagnosis and columns the diagnosis predicted by regional diffusion tensor imaging values of the DRTT and the UPDRS gait and postural stability sum-score. Bold indicates correct diagnosis.

and the disease duration ($r = 0.60$, $p < 0.05$, regression slope: $y = 62x+1113$) as well as the UPDRS gait and postural stability sum-score ($r = 0.67$, $p < 0.05$, regression slope: $y = 29x+956$). No significant correlations were evident of MD values of ROIs and clinical parameters of the PSP-P and PD groups.

3.6. Discrimination among PSP-RS, PSP-P and PD patients (Table 2)

LDA revealed that MD and FA values of the more affected side of the DRTT could classify 11 out of 12 PSP-RS patients (91.7%), 9 out of 12 PSP-P patients (75.0%) and 17 out of 20 PD patients (85.0%) correctly, resulting in an overall correct classification of 84.1% (37 out of 44) (Wilks' Lambda: MD 0.20; FA 0.33 (both $p < 0.001$); Table 2a). The sole use of the UPDRS gait and postural stability sum-score classified 70.5% (31 out of 44) of all subjects correctly (Supplementary Table 6). When adding the UPDRS gait and postural stability sum-score to the DTI values of the DRTT, the overall diagnostic accuracy was improved to 95.5%. 11 out of 12 PSP-RS patients (91.7%), 11 out of 12 PSP-P patients (91.7%) and all PD patients (100%) were classified correctly (Wilks' Lambda: MD 0.20; FA 0.33; UPDRS gait score 0.34 ($p < 0.001$); Table 2b). Only one PSP-P patient was classified into the PD group and one PSP-RS patient was classified into the PSP-P group. Following cross-validation the overall classification error increased from 5 to 6.8%.

4. Discussion

In the present study observer-independent DTI analysis of the DRTT in combination with the UPDRS derived gait and postural stability sum-score provided a highly predictive set of markers yielding an accuracy of 95% for the diagnosis of PSP-P, PSP-RS and PD at initial clinical visit. Consistent with clinico-pathological validation studies of current diagnostic PSP criteria, clinical

Please cite this article in press as: M. Seki, et al., Diagnostic potential of dentatorubrothalamic tract analysis in progressive supranuclear palsy, Parkinsonism and Related Disorders (2018), https://doi.org/10.1016/j.parkreldis.2018.02.004

diagnostic accuracy of PSP-P in our study was only 50% at the first visit and was improved to 91.7% with the help of MRI and the UPDRS gait and postural stability sum-score [4,6,23,24]. Voxel-based analysis revealed alterations of microstructural integrity and corresponding volume loss of various parts of the DRTT including the dentate nucleus, the SCP, the decussation of the SCP and the thalamus were most pronounced in the PSP-RS group and less marked in the PSP-P group. This finding is in line with MRI morphometry, DTI and resting-state functional MRI studies reporting significant volume loss, diffusivity changes and altered functional connectivity of the DRTT or SCP in more advanced disease stages at the group level [12,15,25,26]. Fiber tracts of the DRTT were described to project from the bilateral dentate nucleus in the cerebellum, through the SCP, toward the contralateral ventrolateral and ventroanterior nuclei of the thalamus [27]. DTI alterations and volume loss of the DRTT in our study corresponded with neuropathological observations showing axonal damage comprising loss of myelinated fibers, tau pathology and microgliosis at the common final stage of PSP [28]. Compared to the PD and HC groups, voxel-based analysis localized significant DTI alterations along the entire DRTT of the PSP-RS group, while in the PSP-P group those signal changes were evident only in parts of the DRTT such as the SCP and the dentate nucleus. Significant DTI differences of the DRTT were identified between the PSP-RS and PSP-P groups. However, no significant volumetric differences of the DRTT was evident between both PSP groups, suggesting a superior diagnostic potential of the DTI metrics in the DRTT for the differentiation between PSP-RS and PSP-P.

Subsequently by applying the observer-independent atlas-based delineation of the DRTT to DTI data, 84% of PSP-RS, PSP-P and PD patients were correctly classified by one-way LDA. This finding was in line with recently published sequential classification approaches in more advanced stages of PSP-P and PD reporting diagnostic accuracies of 86% for the ratio of the pons to midbrain area and of 74% for FA signals of the SCP [14,15]. Because of clinical overlap, the severity of gait disturbance and postural instability did not provide enough potential to differentiate among PSP-RS, PSP-P and PD in early to moderately advanced stages. The limited diagnostic potential of the sole use of MRI as well as the moderate sensitivity and positive predictive values of early clinical features led to the concept to investigate the combination of both assessments [19].

In our study the UPDRS gait and postural stability sum-score was significantly more altered in both PSP groups compared to PD and correlated with increased MD values of the more affected side of the DRTT in the PSP-RS group but not in the PSP-P group. This result is consistent with other MRI studies in PSP-RS showing significant correlations between DTI metrics of the SCP/DRTT and clinical measures of gait and balance [26,29]. The interaction of DTI abnormalities of the DRTT and postural instability is likely to correspond to previous observations of an inverse interaction between reduced activation of the thalamus via ascending projections from the mesencephalic tegmentum and higher frequency of falls in PSP patients detected by [^{18}F]FDG PET and functional MRI [30]. When adding the UPDRS gait and postural stability sum-score to the MRI-based model, diagnostic accuracy was improved to 91.7% for PSP-P, to 91.7% for PSP-RS and to 100% for PD.

While most of our findings confirm previous work, there are also important advances with the methods used here. First, SUIT preserves the anatomical details of the infratentorial structures more accurately than the commonly used Montreal Neurological Institute template. By applying voxel-based analysis with the help of a high-resolution infratentorial template to multimodal MRI for the first time, we could identify the clusters with altered DTI signals continuously along the DRTT in PSP-RS. Second, the recently developed probabilistic infratentorial white matter atlas employed in this study is superior in terms of delineation of the entire DRTT including the DSCP [22]. An automated, atlas-based approach for the DRTT allows its observer-independent applicability in clinical practice, which represents an important advance over previous observer-dependent approaches. Finally, we could show that the addition of the UPDRS derived gait and postural stability sum-score significantly enhanced diagnostic accuracy of the MRI-based model.

The lack of definite diagnostic confirmation by neuropathologic assessment is a potential limitation of the current study and misdiagnosis in some of the clinically diagnosed patients cannot be excluded in the absence of postmortem verification. However, clinical diagnoses were based on stringent criteria, and all patients had follow-up clinical investigations of at least 24 months after having completed the imaging study. In addition to the DRTT, the significant voxel-clusters identified by the voxel-to-voxel approach were located to small parts of the cerebellum. Those clusters were not included to the LDA, as dedicated and validated MRI atlases including cerebellar subdivisions or an independent test set of PSP patients were not accessible in order to avoid data overfitting. The diagnostic procedure of combined DTI metrics of the DRTT and clinical assessment of gait and postural stability was evaluated in this proof-of-principle study and should be further validated in independent and larger sample sizes.

5. Conclusion

Voxel-based analysis using a high-resolution infratentorial template identified marked MRI abnormalities localized to the DRTT in PSP-RS and PSP-P, matching the underlying pathological features. Alteration of microstructural integrity of the DRTT in PSP-RS was significantly more pronounced compared to PSP-P and was associated with impairments of gait and postural stability. By applying a validated, observer-independent probabilistic atlas for the DRTT metrics in combination with the UPDRS derived gait and postural stability sum-score, the assignment of a patient to the disease entities of PSP-RS, PSP-P and PD was markedly improved in early to moderately advanced disease stages. Our proposed strategy will be of particular advantage for adequate patient counselling, tailoring appropriate treatments and providing correct diagnosis for patients to be enrolled in clinical studies.

Conflicts of interest

The authors declare that there are no conflicts of interests to report.

Acknowledgments

This study was funded by the Oesterreichische Nationalbank (Austrian Central Bank, Anniversary Fund, project number: 14174), the Austrian Science Fund (FWF: Der Wissenschaftsfonds, project number: KLI82-B00), the Uehara Memorial Foundation and Grants for International Activities in Life Sciences and Medicine, Keio University Medical Science Fund.

Appendix A. Supplementary data

Supplementary data related to this article can be found at https://doi.org/10.1016/j.parkreldis.2018.02.004.

References

[1] J.C. Steele, J.C. Richardson, J. Olszewski, Progressive supranuclear palsy. A

heterogeneous degeneration involving the brain stem, basal ganglia and cerebellum with vertical gaze and pseudobulbar palsy, nuchal dystonia and dementia, Arch. Neurol. 10 (1964) 333–359.
[2] J.J. Hauw, S.E. Daniel, D. Dickson, D.S. Horoupian, K. Jellinger, P.L. Lantos, A. McKee, M. Tabaton, I. Litvan, Preliminary NINDS neuropathologic criteria for Steele-Richardson-Olszewski syndrome (progressive supranuclear palsy), Neurology 44 (11) (1994) 2015–2019.
[3] I. Litvan, J.J. Hauw, J.J. Bartko, P.L. Lantos, S.E. Daniel, D.S. Horoupian, A. McKee, D. Dickson, C. Bancher, M. Tabaton, K. Jellinger, D.W. Anderson, Validity and reliability of the preliminary NINDS neuropathologic criteria for progressive supranuclear palsy and related disorders, J. Neuropathol. Exp. Neurol. 55 (1) (1996) 97–105.
[4] I. Litvan, Y. Agid, D. Calne, G. Campbell, B. Dubois, R.C. Duvoisin, C.G. Goetz, L.I. Golbe, J. Grafman, J.H. Growdon, M. Hallett, J. Jankovic, N.P. Quinn, E. Tolosa, D.S. Zee, Clinical research criteria for the diagnosis of progressive supranuclear palsy (Steele-Richardson-Olszewski syndrome): report of the NINDS-SPSP international workshop, Neurology 47 (1) (1996) 1–9.
[5] D.R. Williams, R. de Silva, D.C. Paviour, A. Pittman, H.C. Watt, L. Kilford, J.L. Holton, T. Revesz, A.J. Lees, Characteristics of two distinct clinical phenotypes in pathologically proven progressive supranuclear palsy: richardson's syndrome and PSP-parkinsonism, Brain : J. Neurol. 128 (Pt 6) (2005) 1247–1258.
[6] G. Respondek, S. Roeber, H. Kretzschmar, C. Troakes, S. Al-Sarraj, E. Gelpi, C. Gaig, W.Z. Chiu, J.C. van Swieten, W.H. Oertel, G.U. Hoglinger, Accuracy of the National Institute for Neurological Disorders and Stroke/Society for Progressive Supranuclear Palsy and neuroprotection and natural history in Parkinson plus syndromes criteria for the diagnosis of progressive supranuclear palsy, Mov. Disord. 28 (4) (2013) 504–509.
[7] I. Litvan, K.P. Bhatia, D.J. Burn, C.G. Goetz, A.E. Lang, I. McKeith, N. Quinn, K.D. Sethi, C. Shults, G.K. Wenning, Movement disorders society scientific issues, movement disorders society scientific issues committee report: SIC task force appraisal of clinical diagnostic criteria for parkinsonian disorders, Mov. Disord. 18 (5) (2003) 467–486.
[8] G. Respondek, M. Stamelou, C. Kurz, L.W. Ferguson, A. Rajput, W.Z. Chiu, J.C. van Swieten, C. Troakes, S. Al Sarraj, E. Gelpi, C. Gaig, E. Tolosa, W.H. Oertel, A. Giese, S. Roeber, T. Arzberger, S. Wagenpfeil, G.U. Hoglinger, The phenotypic spectrum of progressive supranuclear palsy: a retrospective multicenter study of 100 definite cases, Mov. Disord. 29 (14) (2014) 1758–1766.
[9] G.U. Hoglinger, G. Respondek, M. Stamelou, C. Kurz, K.A. Josephs, A.E. Lang, B. Mollenhauer, U. Muller, C. Nilsson, J.L. Whitwell, T. Arzberger, E. Englund, E. Gelpi, A. Giese, D.J. Irwin, W.G. Meissner, A. Pantelyat, A. Rajput, J.C. van Swieten, C. Troakes, A. Antonini, K.P. Bhatia, Y. Bordelon, Y. Compta, J.C. Corvol, C. Colosimo, D.W. Dickson, R. Dodel, L. Ferguson, M. Grossman, J. Kassubek, F. Krismer, J. Levin, S. Lorenzl, H.R. Morris, P. Nestor, W.H. Oertel, W. Poewe, G. Rabinovici, J.B. Rowe, G.D. Schellenberg, K. Seppi, T. van Eimeren, G.K. Wenning, A.L. Boxer, L.I. Golbe, I. Litvan, P.S.P.S.G, Movement Disorder Society-endorsed, Clinical diagnosis of progressive supranuclear palsy: the movement disorder society criteria, Mov. Disord. 32 (6) (2017) 853–864.
[10] A.E. Lang, Clinical heterogeneity in progressive supranuclear palsy: challenges to diagnosis, pathogenesis and future therapies, Mov. Disord. 29 (14) (2014) 1707–1709.
[11] A. Quattrone, G. Nicoletti, D. Messina, F. Fera, F. Condino, P. Pugliese, P. Lanza, P. Barone, L. Morgante, M. Zappia, U. Aguglia, O. Gallo, MR imaging index for differentiation of progressive supranuclear palsy from Parkinson disease and the Parkinson variant of multiple system atrophy, Radiology 246 (1) (2008) 214–221.
[12] F. Agosta, M. Pievani, M. Svetel, M. Jecmenica Lukic, M. Copetti, A. Tomic, A. Scarale, G. Longoni, G. Comi, V.S. Kostic, M. Filippi, Diffusion tensor MRI contributes to differentiate Richardson's syndrome from PSP-parkinsonism, Neurobiol. Aging 33 (12) (2012) 2817–2826.
[13] F. Agosta, V.S. Kostic, S. Galantucci, S. Mesaros, M. Svetel, E. Pagani, E. Stefanova, M. Filippi, The in vivo distribution of brain tissue loss in Richardson's syndrome and PSP-parkinsonism: a VBM-DARTEL study, Eur. J. Neurosci. 32 (4) (2010) 640–647.
[14] G. Longoni, F. Agosta, V.S. Kostic, T. Stojkovic, E. Pagani, T. Stosic-Opincal, M. Filippi, MRI measurements of brainstem structures in patients with Richardson's syndrome, progressive supranuclear palsy-parkinsonism, and Parkinson's disease, Mov. Disord. 26 (2) (2011) 247–255.
[15] G. Nicoletti, M.E. Caligiuri, A. Cherubini, M. Morelli, F. Novellino, G. Arabia, M. Salsone, A. Quattrone, A fully automated, atlas-based approach for superior cerebellar peduncle evaluation in progressive supranuclear palsy phenotypes, AJNR Am J Neuroradiol 38 (3) (2017) 523–530.
[16] K.J. Friston, J. Ashburner, C.D. Frith, J.B. Poline, J.D. Heather, R.S.J. Frackowiak, Spatial registration and normalization of images, Hum. Brain Mapp. 3 (3) (1995) 165–189.
[17] J. Diedrichsen, A spatially unbiased atlas template of the human cerebellum, Neuroimage 33 (1) (2006) 127–138.
[18] A.J. Hughes, S.E. Daniel, L. Kilford, A.J. Lees, Accuracy of clinical diagnosis of idiopathic Parkinson's disease: a clinico-pathological study of 100 cases, J. Neurol. Neurosurg. Psychiatry 55 (3) (1992) 181–184.
[19] D.R. Williams, A.J. Lees, What features improve the accuracy of the clinical diagnosis of progressive supranuclear palsy-parkinsonism (PSP-P)? Mov. Disord. 25 (3) (2010) 357–362.
[20] W.R. Gibb, A.J. Lees, The relevance of the Lewy body to the pathogenesis of idiopathic Parkinson's disease, J. Neurol. Neurosurg. Psychiatry 51 (6) (1988) 745–752.
[21] F. Fazekas, J.B. Chawluk, A. Alavi, H.I. Hurtig, R.A. Zimmerman, MR signal abnormalities at 1.5 T in Alzheimer's dementia and normal aging, AJR Am. J. Roentgenol. 149 (2) (1987) 351–356.
[22] K.M. van Baarsen, M. Kleinnijenhuis, S. Jbabdi, S.N. Sotiropoulos, J.A. Grotenhuis, A.M. van Cappellen van Walsum, A probabilistic atlas of the cerebellar white matter, Neuroimage 124 (Pt A) (2016) 724–732.
[23] I. Litvan, Y. Agid, J. Jankovic, C. Goetz, J.P. Brandel, E.C. Lai, G. Wenning, L. D'Olhaberriague, M. Verny, K.R. Chaudhuri, A. McKee, K. Jellinger, J.J. Bartko, C.A. Mangone, R.K. Pearce, Accuracy of clinical criteria for the diagnosis of progressive supranuclear palsy (Steele-Richardson-Olszewski syndrome), Neurology 46 (4) (1996) 922–930.
[24] Y. Osaki, Y. Ben-Shlomo, A.J. Lees, S.E. Daniel, C. Colosimo, G. Wenning, N. Quinn, Accuracy of clinical diagnosis of progressive supranuclear palsy, Mov. Disord. 19 (2) (2004) 181–189.
[25] J.L. Whitwell, R. Avula, A. Master, P. Vemuri, M.L. Senjem, D.T. Jones, C.R. Jack Jr., K.A. Josephs, Disrupted thalamocortical connectivity in PSP: a resting-state fMRI, DTI, and VBM study, Park. Relat. Disord. 17 (8) (2011) 599–605.
[26] Y. Surova, M. Nilsson, J. Latt, B. Lampinen, O. Lindberg, S. Hall, H. Widner, C. Nilsson, D. van Westen, O. Hansson, Disease-specific structural changes in thalamus and dentatorubrothalamic tract in progressive supranuclear palsy, Neuroradiology 57 (11) (2015) 1079–1091.
[27] J. Voogd, H.K. Feirabend, J.H. Schoen, Cerebellum and precerebellar nuclei, in: G. Paxinos (Ed.), The Human Nervous System, Academic Press, Inc., San Diego, 1990, pp. 321–386.
[28] K. Ishizawa, D.W. Dickson, Microglial activation parallels system degeneration in progressive supranuclear palsy and corticobasal degeneration, J. Neuropathol. Exp. Neurol. 60 (6) (2001) 647–657.
[29] J.L. Whitwell, J. Xu, J. Mandrekar, J.L. Gunter, C.R. Jack Jr., K.A. Josephs, Imaging measures predict progression in progressive supranuclear palsy, Mov. Disord. 27 (14) (2012) 1801–1804.
[30] A. Zwergal, C. la Fougere, S. Lorenzl, A. Rominger, G. Xiong, L. Deutschenbaur, J. Linn, S. Krafczyk, M. Dieterich, T. Brandt, M. Strupp, P. Bartenstein, K. Jahn, Postural imbalance and falls in PSP correlate with functional pathology of the thalamus, Neurology 77 (2) (2011) 101–109.

Please cite this article in press as: M. Seki, et al., Diagnostic potential of dentatorubrothalamic tract analysis in progressive supranuclear palsy, Parkinsonism and Related Disorders (2018), https://doi.org/10.1016/j.parkreldis.2018.02.004